

Reduction of artefacts caused by missing ray-sum data in optical-CT imaging of implants in gel dosimeters

A Asena¹, S T Smith¹, T Kairn^{1,2}, S B Crowe^{1,3}, R D Franich⁴, and J V Trapp¹

¹School of Chemistry, Physics, and Mechanical Engineering, Queensland University of Technology, Brisbane, Australia

²Genesis Cancer Care Queensland, Brisbane, Australia

³Royal Brisbane and Women's Hospital, Brisbane, Australia

⁴School of Science, RMIT University, Melbourne, Australia

E-mail: andre.asena3@gmail.com

Abstract. This study demonstrates the degradation in image quality, and subsequent dose evaluation inaccuracies, that are encountered when an optical-CT system reconstructs an image slice of a gel dosimeter containing an opaque implant, and evaluates the feasibility of a simple correction method to improve the accuracy of radiotherapy dose distribution measurements under these circumstances. MATLAB was used to create a number of different virtual phantoms and treatment plans along with their synthetic projections and reconstructed data sets. The results have illustrated that accurately evaluating 3D gel dose distributions in the vicinity of high-Z interfaces is not possible using the filtered back projection method, without correction, as there are serious artefacts throughout the dose volume that are induced by the missing ray-sum data. Equivalent artefacts were present in physical measurements of irradiated PAGAT gel containers when read by an optical-CT system. An interpolation correction performed prior to reconstruction via the filtered back projection algorithm has been shown to significantly improve dose evaluation accuracy to within approximately 15 mm of the opacity. With careful placement of the implant within the gel sample, and use of the linear interpolation method described in this study, there is the potential for more accurate optical CT imaging of gels containing opaque objects.

1. Introduction

Gel dosimeters show potential for measuring complex radiation dose distributions, particularly in radiotherapy [1-10]. Among the potential applications of gel dosimeters in radiotherapy are those in which the irradiated portion of the gel dosimeter surrounds an imbedded object, such as a metallic implant [11-13], head and neck phantoms [14], inserts for brachytherapy measurements [15], or implanted scintillators [16]. In these cases, options for readout of gel dosimeters are limited; there is significant potential for artefacts in MRI and x-ray CT, and missing data in optical computed tomography (optical-CT) due to opacity of the object.

In this work we investigate a methodology for reconstruction of optical-CT images of gel dosimeters which contain obstructions, thereby removing ray-sum data from projections acquired during imaging. The filtered back projection (FBP) method, which is currently employed in both x-ray CT and optical-CT systems, does not provide a mechanism to deal with incomplete sets of projection data or missing ray-sum data caused by metallic or opaque implants [17]. A number of different reconstruction methods to reduce metal artefacts in x-ray CT have been proposed [18, 19] showing mixed results.



However, these are inapplicable to OCT as ray-sum data is completely removed by opacities, rather than being significantly affected but still present in the case of x-ray CT. Here we evaluate the feasibility of a simple pre-reconstruction correction method to improve the accuracy of gel dosimetry dose distribution measurements under these circumstances.

2. Method

MATLAB (version 8.4.0.150421, R2014b) was used to generate a series of virtual phantoms and treatment plans along with their synthetic projections and reconstructed data sets. This simulated work permitted the exclusion of noise influences and light scattering effects, which allowed effects of missing ray-sum data on the image quality of an optical-CT system to be specifically evaluated. Fig. 1 illustrates how a virtual phantom was forward-projected using the RADON function to produce sinograms, which emulate the result that would be obtained via optical-CT scanning. Removing a defined range from the projection data in each sinogram models the effects of having a completely attenuating object present in the phantom. Sinograms were then reconstructed using the IRADON function for projections sampled at 0.25° intervals, using cubic interpolation, and the Hann window for frequency domain filtering. These parameters were chosen as they match the conditions used for reconstructing data obtained from the MGS Research IQScan optical-CT scanner (MGS Research, Madison, CT, USA).

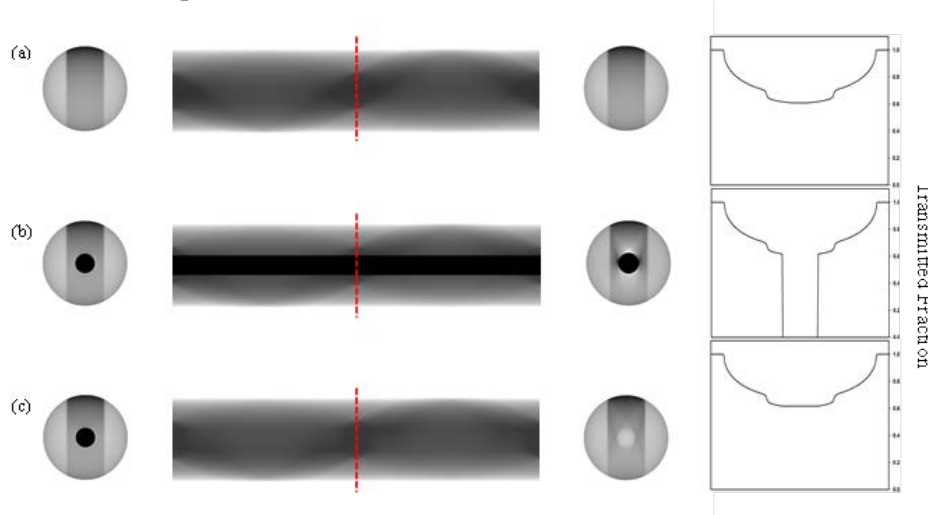


Figure 1. Simulated treatment plans of a circular phantom with a square-field irradiation. Each row of images depicts the original virtual phantom, followed by its forward projected sinogram (with a corresponding profile), and back projected reconstructions. (a) Sinogram with a complete set of ray-sum data, (b) Sinogram with missing ray-sum data, and (c) Sinogram with missing ray-sum data that has been linearly interpolated.

A variety of virtual phantoms were generated to investigate the potential for 3D gel dose distribution measurements for phantoms containing high density implants. Here we simulated a simple 6 MV photon treatment of a circular gel phantom with a high-density, opaque obstruction. The effect of the radiation beam on gel opacity was modelled as a wide, linear region of elevated pixel values passing through the simulated gel cylinder. The falloff of radiation dose (and gel opacity) with depth was modelled as a simple exponential attenuation – a decrease in the pixel values in the region from the top to the bottom of the simulated gel cylinder. Image slices were reconstructed with 1 mm, and 0.25 mm pixel size to investigate the dependence of artefacts on pixel resolution. To highlight the problems associated with dose measurements close to high-Z interfaces, the implant was modelled to reduce the downstream dose by 50%.

The missing ray-sum data was then corrected by linearly interpolating between the data points immediately adjacent to the obstruction for each angular projection. Fig. 1 (a) shows an example of a virtual gel phantom with its forward projected sinogram and back projected reconstruction. Fig. 1 (b) shows a comparable set of simulations for a similar gel phantom that contains an obstruction as

demonstrated by the depleted signal in the central axis of the sinogram. An example of the application of this method is shown in Fig. 1 (c).

A PAGAT polymer gel dosimeter was also prepared as per the recipe recommended by Venning *et al* and Khoei *et al* [20, 21]. When the preparation of the final polymer gel solution was completed, it was transferred into two 7cm diameter, cylindrical containers one of which contained a 1.5cm diameter circular obstruction. The containers were allowed to set for 24 hours by storage in a refrigerator. Irradiations were performed with a 6 MV photon beam from an Elekta linac. 3D dose distributions were read out 24 hours after irradiation, using the MGS Research IQScan optical CT scanner. The data was reconstructed to match results from simulated work using the FBP algorithm with cubic interpolation, and the Hann window for frequency domain filtering. The method of linear interpolation of missing ray-sum data was also applied to this experimental work.

3. Results

The simulated results of photon treatment plans of a circular gel phantom with a high-density obstruction are presented in Fig. 2 (a-c). A 50% downstream dose depletion caused by a high-density implant has been simulated; however, the increased doses caused by lateral-scatter and backscatter were not considered in these simulations. For high-density implant dosimetry, characterising the downstream dose depletion is of paramount importance. These specific conditions were simulated to evaluate the potential for 3D gel dose distribution measurements in the vicinity of high-density implants. Corresponding central axis profile plots in Fig. 2 (d) shows the difference between the true dose distribution and the dose distribution after reconstruction with the FBP algorithm. These profiles are not intended to present estimations of the dose inside the obstruction, but rather the doses in the region of the interface.

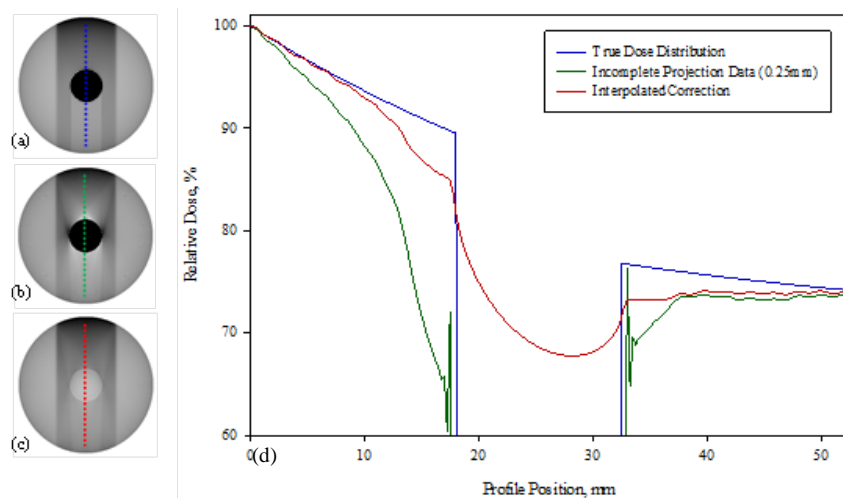


Figure 2. (a) Simulated 6 MV photon treatment plan of a circular gel phantom with opaque, high-density obstruction that reduces the dose by 50%. (b) Image slices have been reconstructed for incomplete sets of projections, (c) and for projection data that has been linearly interpolated, and (d) corresponding central axis profile plot of reconstructed data.

The uncorrected data shows significant artefacts surrounding the obstruction. Relative to the true dose, errors of 24% upstream (17 mm profile position) and 9% downstream (35 mm profile position) are present for the data sets that have been reconstructed using FBP. Applying the linear interpolation reduces the upstream error to 9% and the downstream error to 5%. This correction presents a dramatic improvement in the achievable measurement accuracy of gel dosimeters containing opaque objects.

Fig. 3 (a) displays a raw sinogram with missing ray-sum data obtained from an optical scan of a gel phantom irradiated with a simple 6 MV square photon field. Artefacts caused by reconstructing the

sinogram with incomplete ray-sum data present themselves as bright spots up- and down-stream of the obstruction. Radial streaking artefacts are also present in Fig. 3 (a).

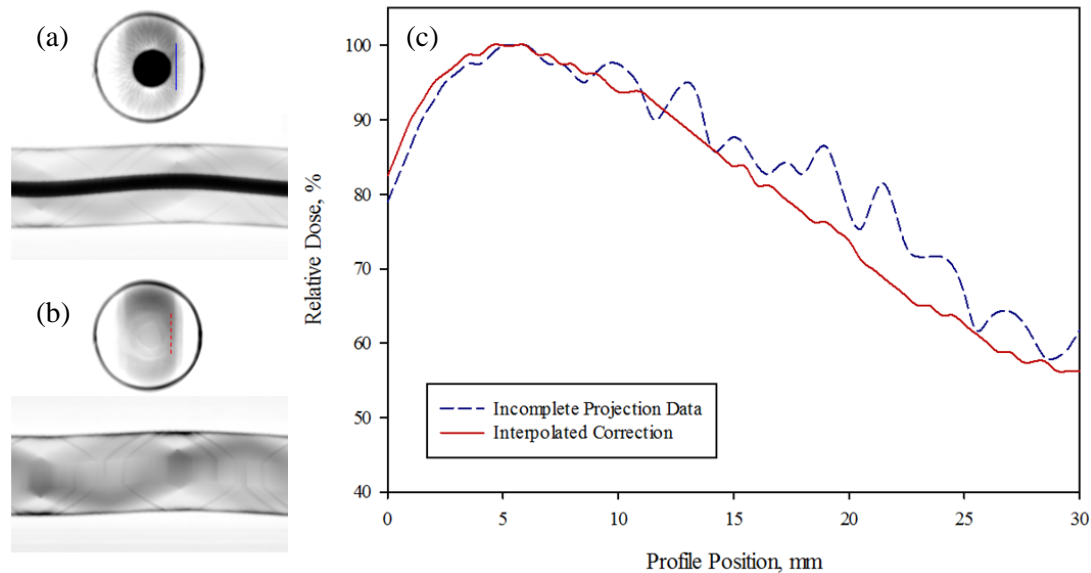


Figure 3. Sinogram and corresponding image reconstructions for a simple square 6MV photon field with an approximately water equivalent obstruction. (a) Image has been reconstructed from sinogram with incomplete ray-sum data, and (b) for data that has been linearly interpolated. (c) Uncorrected vs. interpolated off axis PDD profile plot of experimental dose distribution data.

Fig. 3 (b) shows the result of replacing missing ray-sum data through linear interpolation, with its corresponding percentage depth-dose (PDD) profile plot in Fig. 3 (c). Interpolation of the missing data has successfully minimised the radial streaking artefacts and smoothed the off-axis dose profile displayed in Fig. 3 (c).

4. Conclusions

Use of the FPB algorithm to reconstruct optical CT image slices containing opaque objects can lead to substantial inaccuracies if the effects of missing ray-sum data are not taken into account. However, the measurement uncertainties can be significantly reduced if a simple linear interpolation method is used to correct the sinograms affected by the opaque object. These results represent a dramatic improvement in the achievable measurement accuracy of optical CT readout in the presence of opaque objects. Combined with careful placement of the implant within the gel sample, the linear interpolation method described in this study has the potential to enable the broader and more accurate use of optical CT for the imaging of gels containing opaque objects.

5. References

- [1] Baldock C *et al* 1998 *Phys. Med. Biol.* **43** 695-702
- [2] Baldock C *et al* 2010 *Phys. Med. Biol.* **55** R1-63
- [3] Hill B *et al* 2002 *Phys. Med. Biol.* **47** 4233-46
- [4] Hill B *et al* 2008 *Phys. Med. Biol.* **24** 149-58
- [5] Healy B J *et al* 2003 *Med. Phys.* **30** 2282-91
- [6] Baldock C 2009 *J. Phys.: Conf. Ser.* **164** 012002
- [7] Baldock C 2006 *J. Phys.: Conf. Ser.* **56** 14-22
- [8] Mather M L *et al* 2003 *Ultrasonics* **41** 551-9
- [9] Hill B *et al* 2005 *Med. Phys.* **32** 1589-97
- [10] Davies J B *et al* 2008 *Radiat. Phys. Chem.* **77** 690-96
- [11] Asena A *et al* 2015 *J. Phys.: Conf. Ser.* **573** 012061
- [12] Kairn T *et al* 2013 *J. Phys.: Conf. Ser.* **444** 012108.

- [13] Asena A *et al* 2015 *Physica Medica* **31** 281-85.
- [14] Partridge M *et al* 2006 *Physica Medica* **22** 97-104.
- [15] Hurley C *et al* 2006 *Nucl. Instrum. Methods A* **565** 801-11
- [16] Poole C *et al* 2011 *Australas. Phys. Eng. Sci. Med.* **34** 327-32
- [17] Verburg J M and Seco J 2012 *Phys. Med. Biol.* **57** 2803-18
- [18] Bazalova M *et al* 2007 *Med. Phys.* **34** 2119-32
- [19] Zhang Z *et al* 2011 *Med. Phys.* **38** 701-11
- [20] Venning A J *et al* 2005 *Phys. Med. Biol.* **50** 3875-88
- [21] Khoei S *et al* 2010 *J. Phys.: Conf. Ser.* **250** 012019